Optically and Chemically Controllable Light Flow in Topological Plasmonic Waveguides Based on Graphene Metasurfaces

Y. Wang[1], **J. W. You**[1,2], **Z. Lan**[1], **and N. C. Panoiu**[1]

[1]University College London, Department of Electronic and Electrical Engineering, Torrington Place, WC1E 7JE, London, United Kingdom

[2]Southeast University, State Key Laboratory of Millimeter Waves, No. 2 Southeast University Road, Nanjing, 211189, China

Abstract— In this work, topologically-protected plasmon transport is demonstrated in graphene-based plasmonic crystal waveguides, the main ideas being subsequently applied to optically and chemically controllable nanodevices. In two configurations of topological graphene metasurfaces created by breaking their inversion symmetry, symmetry-protected Dirac cones associated to the underlying metasurfaces are gapped out, which leads to the formation of topological valley modes inside the nontrivial bandgap. The propagation of the corresponding topological modes shows unidirectional characteristics in both cases. Based on the proposed plasmonic topological waveguides, an active optical nanoswitch and a gas molecular sensor are designed by optically and chemically tuning the frequency dispersion of graphene metasurfaces via Kerr effect and gas molecular absorption, respectively. Specifically, the variation of the frequency dispersion of graphene can switch the topological mode into the region of leaky bulk modes, resulting in a dramatic variation of the plasmon transmission. Our work may contribute to the development of new ultracompact and ultrafast active photonic nanodevices based on graphene.

1. INTRODUCTION

Topologically protected edge states with large propagation distance and broadband spectral range are known to be robust against disorder-induced backscattering [1, 2, 3]. Topological photonic modes can emerge inside a nontrivial bandgap, which can be realized by gapping out symmetry-protected Dirac cones[1, 2, 3]. Specifically, the time-inversion-symmetry of the photonic system can be broken by adding an external static magnetic field [4, 5], and the breaking of the spatial-inversion-symmetry can be achieved by dint of spatial perturbations [6, 7]. Most of the previous studies on topological photonics have focused on photonic crystals and linear photonic systems, but applying topological photonics ideas to two-dimensional (2D) photonic materials like graphene, which possesses promising nonlinear optical properties, makes it possible to develop novel integrated ultracompact graphene-based photonic nanodevices [8, 9, 10].

In this work, we present topologically protected plasmon transport in graphene plasmonic waveguides created by breaking the inversion symmetry of two graphene structures: i) a single graphene nanohole metasurface and ii) a bilayer graphene metasurfaces. In both cases, the underlying graphene metasurfaces consist of a hexagonal periodic distribution of air nanoholes in a uniform graphene sheet. By introducing extra nanoholes or by horizontally shifting the top graphene layer, the spatial-inversion-symmetry-protected or mirror-symmetry-protected Dirac cones associated to the two configurations are gapped out, respectively. As a result, topological valley interfacial modes emerge inside the nontrivial bandgap and show unidirectional properties along the domain-wall interface in both cases. Furthermore, based on the strong Kerr effect and chemically-tunable optical property of graphene, an active optical nanoswitch implemented in the single graphene metasurface and a chemically controllable gas molecular sensor implemented in bilayer graphene metasurfaces are investigated. Our computational results quantitatively characterize the high functionality of the optically controllable nanoswitch and the high sensitivity of gas molecular sensor.

2. TOPOLOGICALLY PROTECTED GRAPHENE PLASMONIC WAVEGUIDES

The schematic of a single graphene nanohole metasurface is shown in Fig. 1(a). The graphene nanohole waveguide is constructed by combining two graphene nanohole crystals with a mirror symmetric domain-wall interface. In order to illustrate the hexagonal periodic distribution of air nanoholes, the unit cell of the graphene nanohole metasurface with two kinds of nanoholes with radius R and r is presented in Fig. 1(b). In our simulations, we set the lattice constant of single

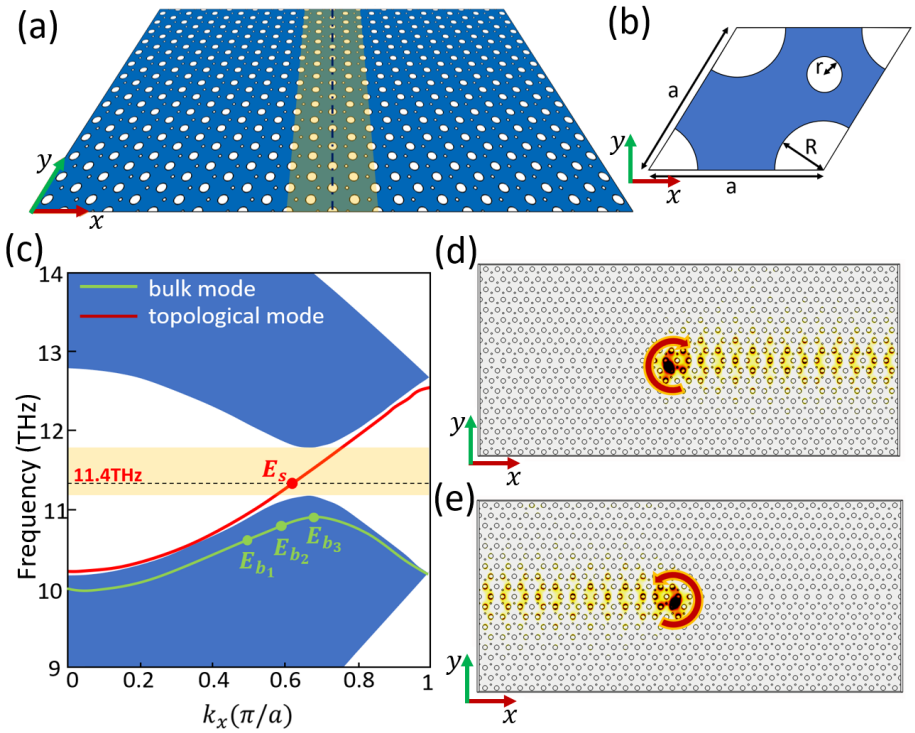

Figure 1: Single graphene nanohole plasmonic waveguide. (a) Schematic of the single graphene nanohole crystal waveguide with a domain-wall interface generated by mirror symmetric left- and right-hand side domains. (b) Unit cell of the single graphene nanohole crystal with lattice constant, a, and two types of nanoholes with radii R and r. (c) Projected band diagram of single graphene nanohole crystal waveguide (blue region), topological valley mode (red line), nontrivial bandgap (yellow region) and bulk mode (green line) determined for extra nanoholes $r = 50\,\text{nm}$. (d) Field distribution of unidirectional topological interfacial mode [E_s at 11.4 THz in Fig. 1(c)] along the positive direction of the x-axis under a left-circular polarized (LCP) source. (e) Field distribution of unidirectional topological interfacial mode along negative x-axis under a right-circular polarized (RCP) source.

graphene nanohole metasurface $a = 400\sqrt{3}$ nm and the radius of nanohole $R = 140\,\text{nm}$. By introducing the smaller nanoholes ($r = 50\,\text{nm}$ in our case), the C_{6v} spatial-inversion symmetry of single graphene nanohole metasurface that protects Dirac cone is broken [11].

In order to identify the topological interfacial mode and nontrivial bandgap, a finite graphene nanohole supercell with a mirror symmetric domian-wall interface is analyzed, and the projected band diagram of single graphene nanohole metasurfaces is shown in Fig. 1(c). We can see that a nontrivial frequency bandgap marked by yellow region is opened in the frequency range from 11.1 THz to 11.8 THz, which is sandwiched by two bulk domains marked by blue regions. More importantly, a topological interfacial mode represented by the red line indeed emerges inside the nontrivial bandgap. Moreover, the unidirectional characteristics of the light propagation of topological interfacial mode E_s in Fig. 1(c) is demonstrated in Fig. 1(d)(e). When the single graphene nanohole plasmonic waveguide is excited by a 11.4 THz left-circular polarized (LCP) source, the light propagation of topological interfacial mode is confined and focused at the domain-wall interface along the positive x-axis. In contrast, the light propagation of topological interfacial mode along the negative x-axis of the domain-wall interface is excited by a 11.4 THz right-circular polarized (RCP) source.

Unlike the configuration of single graphene nanohole metasurface with spatial-inversion symmetry breaking, bilayer graphene plasmonic metasurfaces with a novel mechanism of mirror symmetry breaking between two graphene layers are investigated. The schematic of bilayer graphene plasmonic metasurfaces is given in Fig. 2(a), which is composed of two graphene nanohole crystal layers with a separation distance $h = 90\,\text{nm}$ in z-axis. The left and right half domains of the top layer are horizontally shifted along opposite directions in y-axis with respect to the bottom layer, leading to the formation of a mirror-symmetric domain-wall interface. As shown from the top view of the unit cell of bilayer graphene metasurfaces (Fig. 2(b)), the top and bottom graphene layers consist

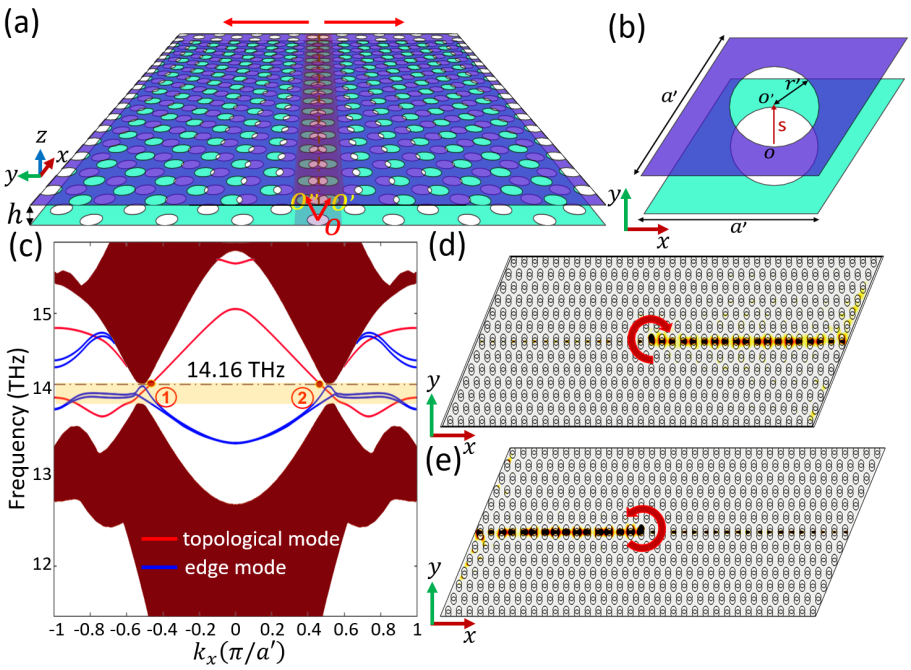

Figure 2: Bilayer graphene plasmonic metasurfaces. (a) Schematic of the bilayer graphene plasmonic metasurfaces with a separation distance h in z-axis. The mirror symmetric domain-wall interface is generated by a horizontal shift between two halves of top layer with respect to the bottom layer along positive and negative y-axis, respectively. (b) Top view of the unit cell of bilayer graphene metasurfaces with the lattice constant, a', and the radius of nanoholes in both layers, r'. The center of the top unit cell O' is horizontally shifted with respect to the center of the bottom unit cell O with a shift distance s. (c) Projected band diagram of bilayer graphene metasurfaces with topological valley mode (red line) and trivial edge modes (blue lines) in the nontrivial bandgap (yellow region), determined for shift distance $s = 100\,\text{nm}$. (d) Unidirectional propagation of topological interfacial mode along the positive x-axis excited by a LCP source, corresponding to ① at 14.16 THz in Fig. 2(c). (e) Unidirectional propagation of topological interfacial mode along the negative x-axis excited by a RCP source, corresponding to ② at 14.16 THz in Fig. 2(c).

of a same nanohole r' etched in a hexagonal lattice. We set the lattice constant of bilayer graphene metasurfaces $a' = 400\,\text{nm}$, the radius of nanohole $r' = 100\,\text{nm}$ and the shift distance $s = 100\,\text{nm}$.

Since the mirror symmetry between two graphene metasurfaces can be broken via a horizontal shift [12], the projected band diagram of bilayer graphene plasmonic metasurfaces is analyzed, and the result is presented in Fig. 2(c). The yellow strip represents the nontrivial bandgap in the frequency range from 13.96 THz to 14.17 THz, and the topological interfacial mode is represented by the red line. Note that the projected band diagram is analyzed based on a finite bilayer graphene supercell, and consequently trivial edge modes marked by blue lines can also emerge inside the bandgap. At the chosen frequency 14.16 THz, the frequency line only crosses the topological band at two points ① and ② inside the bandgap. These two points have opposite k vectors and sign of the slope of their dispersion curves, which can lead to corresponding light propagation in opposite directions along the domain-wall interface as shown in Fig. 2(d)(e). When a LCP and a RCP excitation source at 14.16 THz are placed in the center of the bilayer graphene plasmonic waveguide, the light of excited topological interfacial mode is highly confined and propagates along the positive (point ①) and negative (point ②) x-axis, respectively.

3. OPTICALLY AND CHEMICALLY CONTROLLABLE NANODEVICES

The unidirectional characteristics of topological interfacial mode in both proposed graphene configurations has great potential on the development of novel nanodevices. In this work, an active optically controllable nanoswitch and a chemically controllable gas molecular sensor are investigated, based on the single graphene nanohole waveguide and the bilayer graphene plasmonic metasurfaces, respectively. As a promising material with large nonlinear refractive index and tunable chemical potential [13, 14], graphene plays a significant role in tuning the refractive index of the whole photonic system, resulting in the shift of frequency dispersion of graphene metasurfaces, especially the

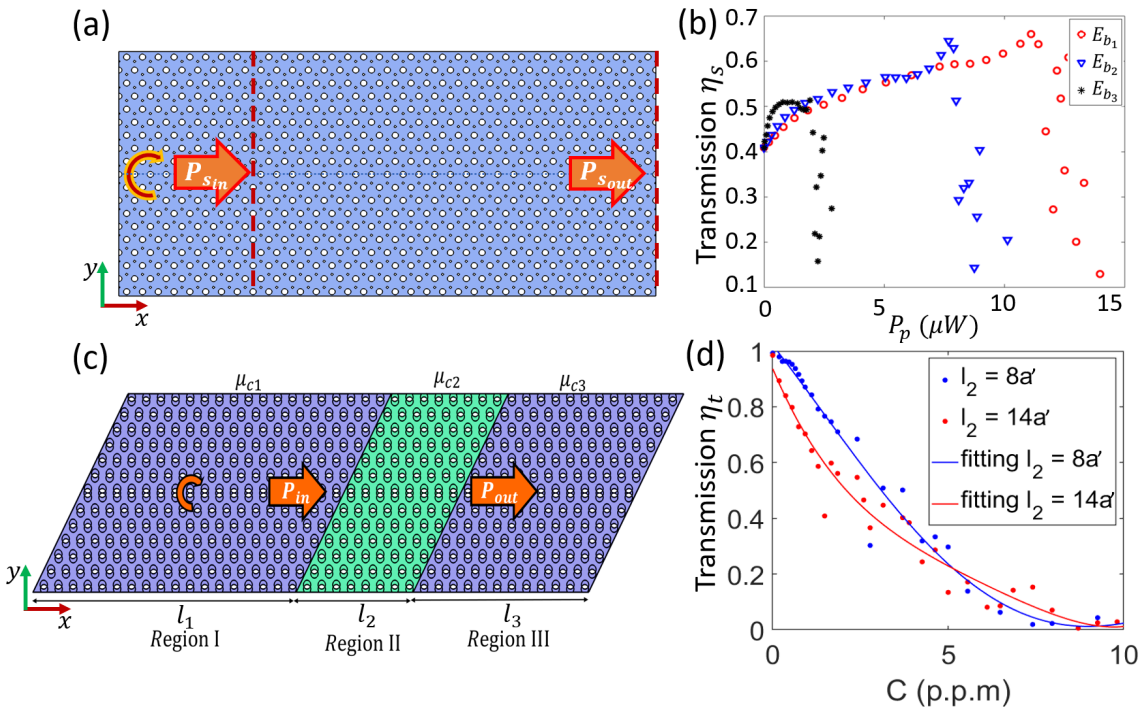

Figure 3: (a) Schematic of the optically controllable nanoswitch based on the single graphene nanohole plasmonic crystal waveguide. The input power $P_{s_{in}}$ and the output power $P_{s_{out}}$ of the signal beam excited by a LCP source at 11.4 THz are measured under the pump of a bulk mode E_b (blue region). (b) Transmission η_s of signal beam with respect to the variation of pump power P_p under the cases pumped by three bulk modes with different group velocities in Fig. 1(c). (c) Schematic of the chemically controllable gas molecular sensor implemented in the bilayer graphene plasmonic metasurfaces, which is composed of three bilayer regions. The middle region II is used to absorb the gas molecules (NO_2) in order to realize the chemical doping. The input power P_{in} and the output power P_{out} of the topological interfacial mode are collected under a LCP excitation source at 14.16 THz. (d) Transmission η_t of the topological interfacial mode with respect to the concentration C of NO_2 gas molecules in the environment, determined for different lengths of region II.

positions of nontrivial bandgap and topological interfacial mode.

In the case of the topological waveguide based on single graphene nanohole metasurface, an active optically controllable nanoswitch is schematized in Fig. 3(a). Based on the strong Kerr effect in graphene, the whole graphene nanohole platform is uniformly pumped by a bulk mode with high power, which can optically change the index of refraction of the system. A topological interfacial mode is excited as the signal beam by a 11.4 THz LCP source and carries the input power $P_{s_{in}}$ and output power $P_{s_{out}}$. When the frequency dispersion of the topological waveguide is tuned via the pump beam, the signal beam can be switched from a topological mode into a leaky bulk mode, resulting in a dramatic decrement of the transmission $\eta_s = P_{s_{out}}/P_{s_{in}}$ of the signal beam. As shown in Fig. 3(b) determined for three bulk modes [E_{b_1}, E_{b_2} and E_{b_3} in Fig. 1(c)] approaching to slow-light regime, the transmission of signal beam is sharply decreased to 0.1 when the increasing pump power P_p reaches the threshold. These results indeed realize an active optically controllable nanoswitch. Specifically, the required switching pump power of E_{b_3} at slow-light regime is up to 5 times smaller than other two bulk modes.

Based on the unidirectional properties on the bilayer graphene plasmonic waveguide, a chemically controllable gas molecular sensor is designed as shown in Fig. 3(c). The sensor is composed of three bilayer regions, where region II is used to detect the NO_2 gas concentration C in the environment. The lengths of three regions are l_1, l_2, and l_3, respectively, and the corresponding initial chemical potentials are $\mu_1 = \mu_2 = \mu_3 = 0.2$ eV. Based on the fact that the chemical potential of graphene can be tuned via NO_2 gas molecular absorption, namely chemical doping, the frequency dispersion of the region II is chemically controlled by the NO_2 gas concentration. When a topological mode is excited by a 14.16 THz LCP source in region I, the variation of the frequency dispersion of region II can switch the topological interfacial mode into a leaky bulk mode. Consequently, the

variation of plasmon transmission $\eta_t = P_{out}/P_{in}$ can precisely indicate the NO_2 gas concentration in the environment, and the result determined for different lengths of region II is demonstrated in Fig. 3(d). The plasmon transmission steeply decreases to zero when more NO_2 gas molecules are absorbed in region II. Our computational results also prove that the longer the length of region II is, the larger the slope of transmission curve is.

4. CONCLUSION

We proposed optically and chemically controllable valley-Hall topological plasmon transport in single graphene nanohole plasmonic waveguides and bilayer graphene plasmonic metasurfaces, respectively, which is further applied on an active optical nanoswitch and an efficient gas molecular sensor. Specific nanoholes are etched so as to break the spatial-inversion symmetry of the single graphene nanohole plasmonic crystal and a horizontal shift is introduced to break the mirror symmetry of the bilayer graphene metasurface, which in both cases results in a gapped-out Dirac cone and topological interfacial mode with unidirectional properties. Based on graphene platform with large nonlinear refractive index and tunable chemical potential, the variation of plasmon transmission on the proposed topological photonic systems is strongly dependent on pump power and NO_2 gas concentration, which indeed realizes an active optically controllable nanoswitch and a chemically controllable gas molecular sensor.

ACKNOWLEDGMENT

This work is funded by China Scholarship Council (CSC) and University College London (UCL).

REFERENCES

1. Lu, L., Joannopoulos, J. D. and Soljacic, M. "Topological photonics," *Nature Photon.*, Vol. 8, No. 11, 821–829, 2014.
2. Lu, L., Joannopoulos, J. D. and Soljacic, M. "Topological states in photonic systems," *Nature Phys.*, Vol. 12, No. 7, 626–629, 2016.
3. Ozawa, T. *et al.* "Topological photonics," *Rev. Mod. Phys.*, Vol. 91, No. 1, 2019, Art. no. 015006.
4. Wang, Z., Chong, Y., Joannopoulos, J. D. and Soljacic, M. "Observation of unidirectional backscattering-immune topological electromagnetic states," *Nature.*, Vol. 461, No. 7265, 772–775, 2009.
5. Poo, Y., Wu, R. X., Lin, Z., Yang, Y. and Chan, C. T. "Experimental realization of self-guiding unidirectional electromagnetic edge states," *Phys. Rev. Lett.*, Vol. 106, No. 9, 2011, Art. no. 093903.
6. Wu, L. H. and Hu, X. "Scheme for achieving a topological photonic crystal by using dielectric material," *Phys. Rev. Lett.*, Vol. 114, No. 22, 2015, Art. no. 223901.
7. Kang, Y., Ni, X., Cheng, X., Khanikaev, A. B.and Genack, A. Z. "Pseudo-spin–valley coupled edge states in a photonic topological insulator," *Nat. Commun.*, Vol. 9, No. 1, 1–7, 2018.
8. Lan, Z., You, J. W. and Panoiu, N. C. "Nonlinear one-way edge-mode interactions for frequency mixing in topological photonic crystals," *Phys. Rev. B.*, Vol. 101, No. 15, 2020, Art. no. 155422.
9. Mittal, S., Goldschmidt, E. A. and Hafezi, M. "A topological source of quantum light," *Nature.*, Vol. 561, No. 7724, 502–506, 2018.
10. Lan, Z., You, J. W., Ren, Q., Sha, Wei E. I. and Panoiu, N. C. "Second-harmonic generation via double topological valley-Hall kink modes in all-dielectric photonic crystals," *Phys. Rev. A.*, Vol. 103, No. 4, 2021, Art. no. L041502.
11. You, J. W., Lan, Z., Bao, Q. and Panoiu, N. C. "Valley-Hall topological plasmons in a graphene nanohole plasmonic crystal waveguide," *IEEE J. Sel. Top. Quantum Electron.*, Vol. 26, No. 6, 1–8, 2020.
12. Wang, Y., You, J. W., Lan, Z. and Panoiu, N. C. "Topological valley plasmon transport in bilayer graphene metasurfaces for sensing applications," *Opt. Lett.*, Vol. 45, No. 11, 3151–3154, 2020.
13. You, J. W., Bongu, S. R., Bao, Q. and Panoiu, N. C. "Nonlinear optical properties and applications of 2D materials: Theoretical and experimental aspects," *Nanophotonics.*, Vol. 8, No. 1, 63–97, 2018.
14. Yao, X. and Belyanin, A. "Giant optical nonlinearity of graphene in a strong magnetic field," *Phys. Rev. Lett.*, Vol. 108, No. 25, 2012, Art. no. 255503.